



Rapid Communication

On saturation suppression in adaptive vibration control

Zhiyi Zhang*, Fang Hu, Junfang Wang

Institute of Vibration, Shock and Noise, Shanghai Jiaotong University, Shanghai 200240, PR China

ARTICLE INFO

Article history:

Received 31 May 2009

Received in revised form

19 September 2009

Accepted 23 November 2009

Handling Editor: L.G. Tham

ABSTRACT

An anti-saturation scheme is presented for adaptive vibration control with LMS controllers. A new recursive formula for weight updating is derived from the optimization of certain object functions, which is an extension of the normalized LMS algorithm. The anti-saturation formula is capable of suppressing controller output in case of a large disturbance and expected to improve the performance of the controller. Numerical simulation and experiment have been conducted to demonstrate the performance of the anti-saturation scheme and the results have shown that the scheme is effective in alleviating output saturation and as a result improves performance of the controller in vibration suppression.

Crown Copyright © 2009 Published by Elsevier Ltd. All rights reserved.

1. Introduction

In real applications, the hybrid passive/active isolation is a preferred way to attenuate vibration transmission, which has the advantages of both passive isolation at high frequencies and active isolation at low frequencies [1,2]. When the disturbing forces/moments are periodic or pseudo-periodic, the spectra of structural vibration are mainly composed of spaced lines. For this type of vibration, the parameter-insensitive adaptive control methods (i.e. narrowband methods) are most effective. Adaptive cancellation is one of the adaptive strategies that can cancel vibration and sound signals of dominant periodic components. The LMS-based algorithms, such as FxLMS, are attractive in real applications for the advantages of fast computation and easy implementation. LMS controllers are applied independently or in combination with tracking filters to control vibration and noise, and particularly used in the control of low frequency vibration as well as sound radiation of thin plates, where the vibration control involves fluid-structure interaction [3–7]. In the control of vibration transmission, the multi-channel adaptive control methods with enhanced LMS algorithm have been experimented in real time control [8]. For a LMS controller that adjusts weights according to a linear updating law, large disturbance will definitely lead to large variations in the controller output. In this circumstance, saturation will occur in the output and consequently induce high frequency excitation on structures and even instability in the controlled system. Therefore, during the implementation of adaptive control, controller saturation should be considered in advance so that the performance of the controlled system is guaranteed even under large disturbance. So far, anti-saturation schemes for general control systems are investigated extensively in the area of nonlinear control, and some of which can be applied to the control of structural vibration [9]. However, there is currently no method that deals with saturation in LMS controllers although saturation is sometimes a serious problem.

In this paper, output saturation is discussed for the LMS-based controllers and an anti-saturation formula for weight updating is derived by the extension of the existing normalized LMS algorithm through optimization. Three sections are organized in the following discussion. The derivation of the new recursive formula is presented in Section 2, and the new

* Corresponding author.

E-mail address: chychang@sjtu.edu.cn (Z. Zhang).

algorithm is demonstrated by a numerical example as well as an experiment in Section 3. Finally, conclusions are given in Section 4.

2. Mathematical description

Fig. 1 is the diagram of an adaptive control system with saturation in the controller output. In the figure, $H(z)$ is the transfer function of the plant, $\hat{H}(z)$ the identified model of the plant, $u(k)$ the saturated output, $e(k)$ the cancelled response, $r(k)$ the reference signal, $x(k)$ the filtered reference signal, $f(k)$ the disturbance force, $d(k)$ the response induced by $f(k)$, $W(z)$ the transfer function of the controller, which is in fact an FIR (finite impulse response) filter, AS-LMS the LMS algorithm with anti-saturation scheme, $H_1(z)$ and $H_2(z)$ are the transfer functions of the reference and the disturbance channels, respectively.

For the simplicity of deduction, assume that $H(z) = 1$. The recursive relation for weight updating can be given by Eq. (1) according to the deepest descent method [10]:

$$w_{k+1} = w_k + \beta e_k x_k \tag{1}$$

where $e_k = d_k - w_k^T x_k$, β is the step-size parameter. Eq. (1) is obtained by the unconstraint optimization that minimizes the instantaneous squared error $J = (d - w_k^T x_k)^2$. Now, in order to consider saturation in the output $u = f(w_k^T x_k)$, additional conditions should be imposed, where $f(\cdot)$ is a sigmoid function. Assume that the recursive relationship can be recast as $w_{k+1} = \alpha w_k + \beta e_k x_k$, where α and β are determined according to certain constraint conditions.

(1) Determine α .

When a strong disturbance occurs in the response signal, $u = w_k^T x_k$ will surpass the output limit of the controller if weights are updated according to Eq. (1). Therefore, the following two conditions are imposed.

- (i) The updated w_{k+1} renders no saturation under the current reference signal x_k , i.e. $w_{k+1}^T x_k = f(w_{k+1}^T x_k)$;
- (ii) $w_{k+1}^T x_k$ approaches $f(w_k^T x_k)$ to the most, and especially $w_{k+1}^T x_k = w_k^T x_k$ when no saturation occurs.

Construct an object function $J_\alpha = (w_{k+1}^T x_k - f(w_k^T x_k))^2$, the above two conditions lead to

$$\frac{\partial J_\alpha}{\partial w_{k+1}} = 2(w_{k+1}^T x_k - f(w_k^T x_k)) \left(1 - \frac{f_u}{\alpha}\right) x_k, \tag{2}$$

where $f_u = \partial f / \partial u$. Therefore, $\partial J_\alpha / \partial w_{k+1} = 0$ yields $\alpha = f_u$.

(2) Determine β .

Construct an object function $J_\beta = \tilde{e}_k^2$, where $\tilde{e}_k = d_k - w_{k+1}^T x_k$ is the expected error. The condition for β is that it should minimize J_β . Therefore, let

$$\frac{\partial J_\beta}{\partial \beta} = 2x_k^T x_k e_k (\Delta w^T x_k - e_k) = 0, \tag{3}$$

where $\Delta w = w_{k+1} - w_k = (f_u - 1)w_k + \beta x_k e_k$, one can have

$$\beta = \frac{e_k + (1 - f_u)w_k^T x_k}{x_k^T x_k e_k}. \tag{4}$$

(3) Relationship between $e_k = d_k - w_k^T x_k$ and $e_k^* = d_k - f(w_k^T x_k)$.

Given the optimal weight vector w_k , the difference between e_k^2 and e_k^{*2} should be minimized. Therefore, the squared error $\Delta e_k^2 = (e_k^{*2} - e_k^2)^2$ reaches its minimum for w_k , that is

$$\frac{\partial \Delta e_k^2}{\partial w_k} = 4\Delta e_k (e_k^* f_u - e_k) x_k = 0 \tag{5}$$

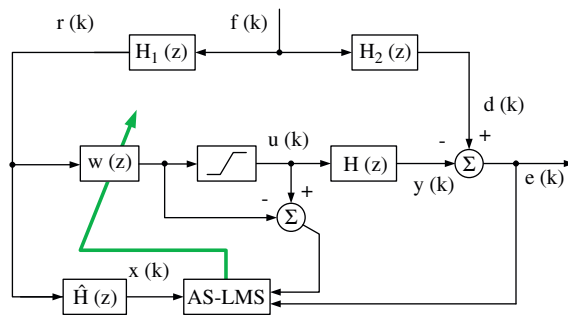


Fig. 1. Adaptive control with controller saturation.

which implies the relationship $e_k = e_k^* f_u$. As a result, the final form of the recursive formula can be written as

$$w_{k+1} = f_u w_k + \frac{f_u e_k^* + (1 - f_u) w_k^T x_k}{x_k^T x_k} x_k \tag{6}$$

By introducing parameters $\mu \in (0, 1)$ and $\gamma > 0$ to Eq. (6) as in the normalized LMS algorithm, one can have

$$w_{k+1} = f_u w_k + \mu \frac{f_u e_k^* + (1 - f_u) w_k^T x_k}{\gamma + x_k^T x_k} x_k \tag{7}$$

It can be seen that Eq. (7) reduces to the normalized LMS algorithm as $f_u = 1$, and as the controller's output is in deep saturation, i.e. $f_u \rightarrow 0$, $w_{k+1} \rightarrow (\mu x_k^T x_k / \gamma + x_k^T x_k) w_k < \mu w_k$.

3. Verification

3.1. Numerical simulation

Fig. 2 is the model used in simulation, which represents mechanical systems that are excited by running machinery and controlled by passive/active mounts inserted between the base structure and the vibration source. Such systems can be met in active suspension of vehicle motors as well as ship engines, etc. In this model, a plate is suspended by four rubber isolators at its four corners. Dimensions of the plate are $0.8\text{ m} \times 0.8\text{ m} \times 0.03\text{ m}$, and mass density of the material is 7850 kg/m^3 , $k_s = 1.81 \times 10^6\text{ N/m}$, $M = 3\text{ kg}$, $k = 3.42 \times 10^4\text{ N/m}$. The control force of the actuator acts on both the mass and the plate, and the measured FRF between the transducer response at the plate center and the input excitation voltage to the actuator is shown in Fig. 3. The first two natural frequencies correspond to the suspension frequencies of the mass and the plate, respectively. Flexible modes of the plate have much higher frequencies than the first two.

The disturbance force is composed of two harmonic components, i.e.

$$F_d = \sin(240\pi t) + 5 \sin(20\pi t) a(t) \tag{8}$$

where $a(t)$ is defined as

$$a(t) = \begin{cases} 1, & t \in [t_1, t_2] \\ 0, & \text{otherwise} \end{cases}$$

Therefore, the low frequency disturbance only exists in a finite duration. The component of 120 Hz is used to simulate the excitation of a machine that works continuously while the component of 10 Hz represents another machine that works

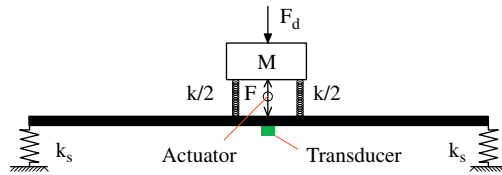


Fig. 2. A flexible vibration model for active isolation.

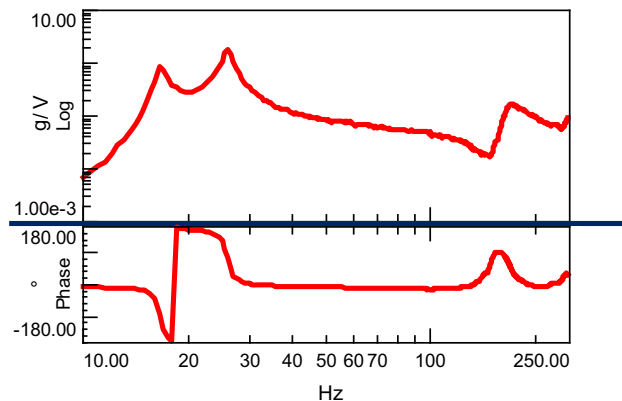


Fig. 3. Magnitude of the FRF.

intermittently. The existence of this intermittent disturbance may cause saturation in the output if the controller does not respond properly in this circumstance. In the simulation, the output limits of the controller are set to ± 1.5 V. First, turn on the anti-saturation scheme and let the intermittent disturbance act within a short time period when the controller works normally. As shown in Figs. 4–6(a), the acceleration response is reduced and no saturation occurs in the output although the controller output is bounded. The controller weights decrease sharply as the initial shock occurs due to the loading of the low frequency disturbance (Fig. 5a). It is this fast shrinkage of weights in response to the instantaneous saturation that guarantees that the controller output does not surpass the limits after loading of the low frequency disturbance (Fig. 6a). For comparison, let the anti-saturation scheme turned off and restart the low frequency disturbance at certain time. The results are shown in Figs. 4–6(b). As can be seen, the controller gets into saturation after the loading of the low frequency disturbance and vibration at the plate center deteriorates during and after the existence of the disturbance (Fig. 4b). Moreover, the controller weights do not change properly in this case, resulting in a continuous saturation in the controller output (Figs. 5b and 6b). It should be noted that the disturbance given in Eq. (8) is not particularly related to system parameters, and the observed phenomenon is determined completely by the adaptive scheme. Similar results can be obtained when the disturbance of different frequencies is used in the simulation. However, the results herein are limited to those shown in Figs. 4–6 so as to avoid a cumbersome description.

Performance of the anti-saturation scheme can be demonstrated further by experiments. However, only one test item has been conducted so far on a test rig, and sufficient verification will be carried out in future investigation.

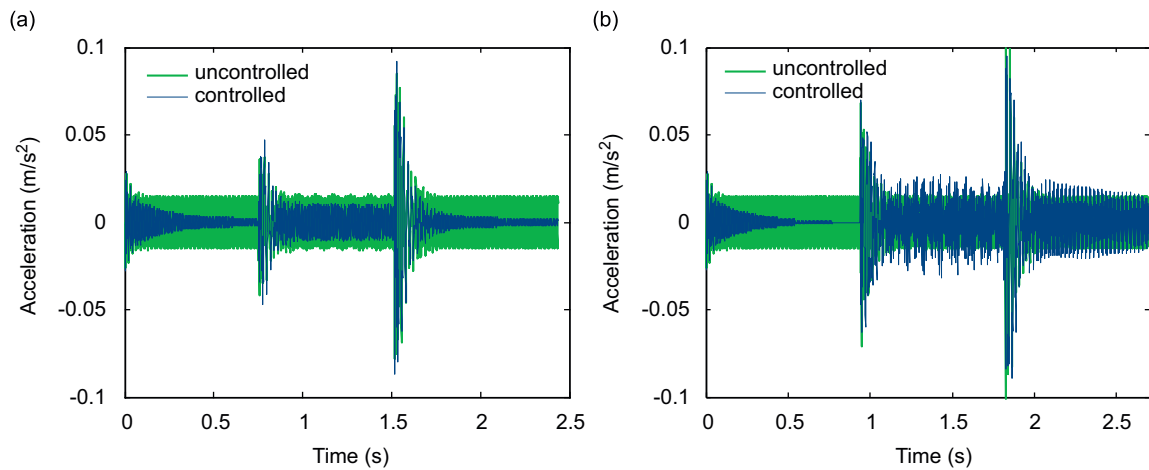


Fig. 4. Acceleration at the plate center without control (Green) and with control (Blue). (a) Saturation controlled; (b) saturation uncontrolled. (For interpretation of the references to color in this figure legend, the reader is referred to the web version of this article.)

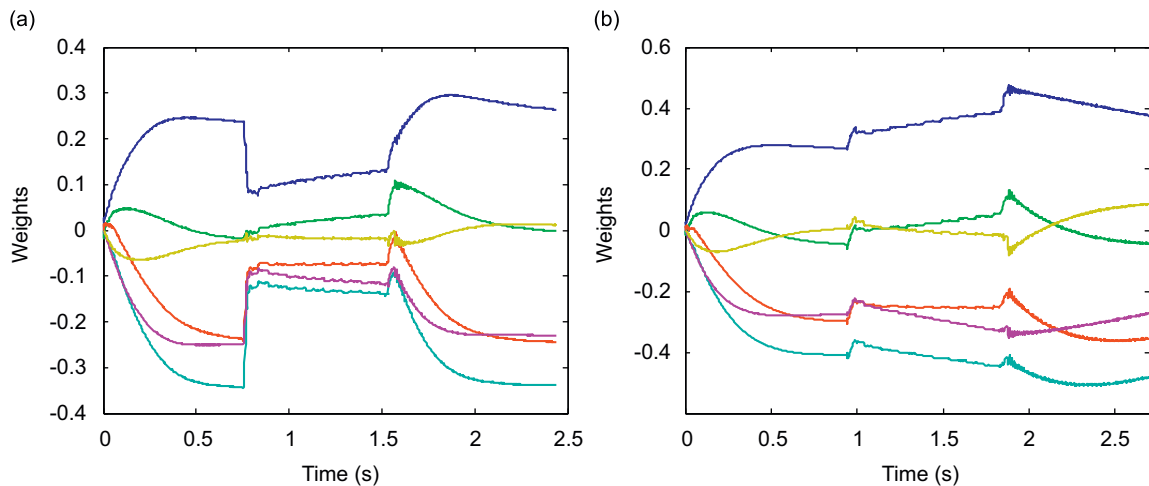


Fig. 5. Weights of the adaptive controller. (a) Saturation controlled; (b) saturation uncontrolled.

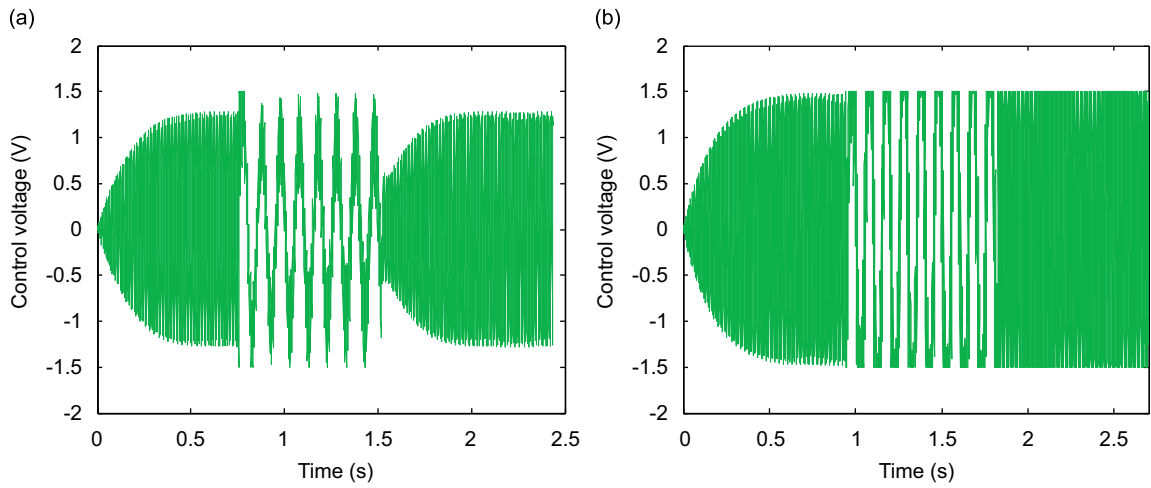


Fig. 6. Output of the adaptive controller. (a) Saturation controlled; (b) saturation uncontrolled.

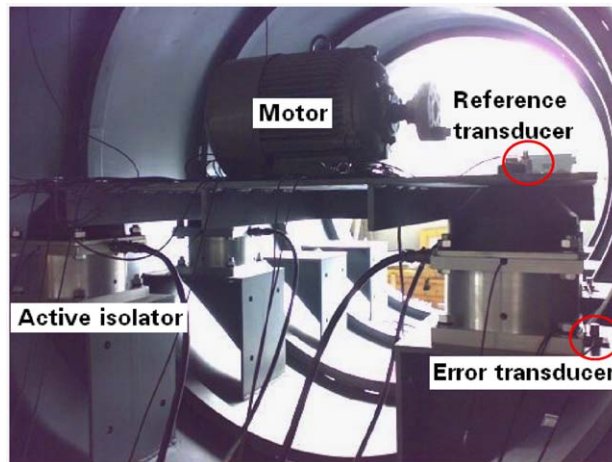


Fig. 7. Test rig for active vibration isolation.

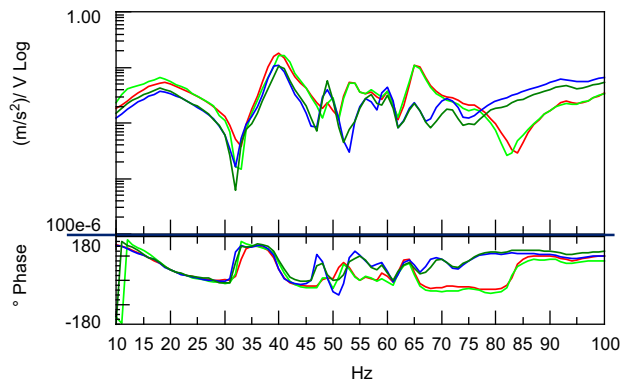


Fig. 8. FRFs of the four control channels.

3.2. Experiment

Fig. 7 is the test rig used for experiments on active vibration isolation. In the test rig, four active isolators are used to isolate the transmission of vibration from the motor to the base structure, on which the isolators are mounted. Moreover,

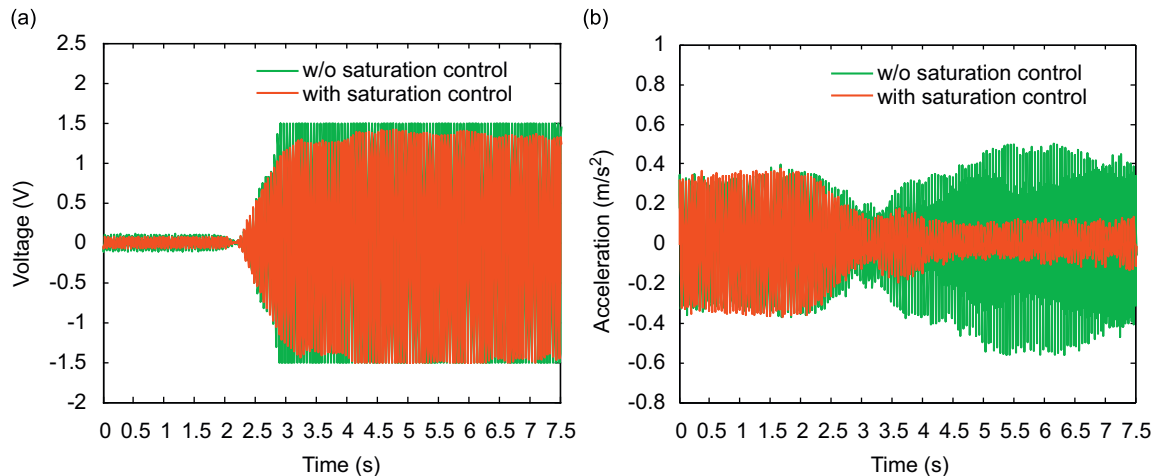


Fig. 9. Error and control signals of one channel under different adaptation schemes of weights. (a) Control signals; (b) error signals.

four error transducers are installed on the base structure and one reference transducer is placed beside the motor. For this system, the adaptive control structure in Fig. 1 is experimented. Fig. 8 shows the FRFs of the four control channels. In the experiment, the excitation frequency of the motor is set to 20 Hz.

The output limits of the controller were set to ± 1.5 V manually in order to create saturation under a relatively small disturbance. Fig. 9 gives the results corresponding to two cases where the anti-saturation scheme was turned on and off, respectively. In Fig. 9, the control action is turned on at about 2.2 s, and after one second or so, output of the controller without anti-saturation scheme gets into saturation, and the error vibration starts to rise. On the contrary, the output of the controller with anti-saturation scheme never gets into saturation and the error vibration is still reduced. This simple experiment has clearly exhibited that saturation in the controller can worsen the performance of isolation, and the suppression of saturation can prevent a long-term overload in the control action.

4. Conclusions

In the implementation of active vibration control, saturation in controller output should be considered. To suppress output saturation, an anti-saturation scheme is introduced to the normalized LMS algorithm and demonstrated effective through a numerical simulation and an experiment on a test rig. The recursive formula for weight updating is derived on certain assumptions that prevent a controller from getting into saturation and guarantee fast convergence of errors in an optimal sense. Therefore, adaptation of an adaptive controller to strong disturbance can be enhanced by the introduction of this anti-saturation scheme.

Acknowledgment

This work was fully supported by the NSF of China (Grant no. 10672099).

References

- [1] S. Daley, F.A. Johnson, J.B. Pearson, R. Dixon, Active vibration control for marine applications, *Control Engineering Practice* (12) (2004) 465–474.
- [2] S. Daley, J. Hatonen, D.H. Owens, Active vibration isolation in a “smart spring” mount using a repetitive control approach, *Control Engineering Practice* (14) (2006) 991–997.
- [3] S.J. Elliott, I.M. Stothers, P.A. Nelson, A multiple error LMS algorithm and its application to the active control of sound and vibration, *IEEE Transactions on Acoustics, Speech, and Signal Processing* 35 (10) (1987) 1423–1434.
- [4] S. Kim, Y. Park, On-line fundamental frequency tracking method for harmonic signal and application to ANC, *Journal of Sound and Vibration* 241 (4) (2001) 681–691.
- [5] S. Kim, Y. Park, Active control of multi-tonal noise with reference generator based on on-line frequency estimation, *Journal of Sound and Vibration* 227 (3) (1999) 647–666.
- [6] B. Mazeaud, M.A. Galland, A multi-channel feedback algorithm for the development of active liners to reduce noise in flow duct applications, *Mechanical Systems and Signal Processing* (21) (2007) 2880–2899.
- [7] Z. Zhang, Y. Chen, X. Yin, H. Hua, Active vibration isolation and underwater sound radiation control, *Journal of Sound and Vibration* (318) (2008) 725–736.
- [8] P. Belanger, A. Berry, Y. Pasco, et al., Multi-harmonic active structural acoustic control of a helicopter main transmission noise using the principal component analysis, *Applied Acoustics* 70 (1) (2009) 153–164.
- [9] A.R. Teel, L. Zaccarian, J.J. Marcinkowski, An anti-windup strategy for active vibration isolation systems, *Control Engineering Practice* (14) (2006) 17–27.
- [10] S. Haykin, *Adaptive Filter Theory*, Prentice Hall, New York, 2001.